



# Solvent effect over the promoter addition for a supported NiWS hydrotreating catalyst

Luis G. Woolfolk<sup>a</sup>, Christophe Geantet<sup>b</sup>, Laurence Massin<sup>b</sup>, Dorothée Laurenti<sup>b</sup>, José A. De los Reyes<sup>a,\*</sup>

<sup>a</sup> Universidad Autónoma Metropolitana Iztapalapa, Av. San Rafael Atlixco 186, México, D.F., 09340, México

<sup>b</sup> Institut de Recherches sur la Catalyse et l'Environnement de Lyon, 2 Albert Einstein Villeurbanne, 69100, France



## ARTICLE INFO

### Article history:

Received 10 March 2016

Received in revised form 16 June 2016

Accepted 29 July 2016

Available online 30 July 2016

### Keywords:

NiWS

Nickel acetylacetone

4,6-Dimethylbenzothiophene

Solvent effect

HDS

## ABSTRACT

A series of NiWS catalysts supported on alumina was synthesized using a reflux of nickel acetylacetone  $\text{Ni}(\text{acac})_2$  solution over previously impregnated and sulfided tungsten. Methanol, isopropanol, acetone and toluene were used as solvents in the incorporation of Ni. The catalysts were tested in the Hydrodesulfurization of 4,6 dimethylbenzothiophene and compared with a conventional NiWS/Al<sub>2</sub>O<sub>3</sub> catalyst (prepared from  $\text{Ni}(\text{NO}_3)_2$ ). UV-vis spectroscopy results showed that the interaction between the nickel atom and its environment was affected in relation to the solvent used. The  $\text{Ni}(\text{acac})_2$  based catalysts showed up to a 3-fold increase in the reaction rate when compared with the reference catalyst. Among the solvents in the impregnation of the metal complex, methanol induced the highest specific activity, 130% higher than the catalyst prepared using toluene. XPS analyses indicated that up to 100% of the methanol-added nickel was forming the decorated "NiWS" active phase.

© 2016 Elsevier B.V. All rights reserved.

## 1. Introduction

In order to produce ultraclean middle distillates, several improvements of the refining processes have been undertaken. Hydrotreating (HDT) units use Mo or W-based catalysts usually supported on alumina. However, more stringent environmental regulations in several countries have motivated the search of more active and selective catalysts [1]. Ni-promoted tungsten sulfide catalysts are known to be more hydrogenating as compared to Mo based catalyst in HDT reactions [1–5]. This property can be exploited to achieve an ultra-deep desulfurization of middle distillates via the hydrogenation of refractory compounds such as 4,6-dimethylbenzothiophene. An important obstacle in the synthesis of Ni(Co) promoted MoS<sub>2</sub> (WS<sub>2</sub>) catalysts lies on the difference between the sulfidation temperatures of both metals [6]. This promotion is relevant to synthesize the mixed "NiWS" phase, which has been recognized to be the active phase of supported NiW sulfide catalysts, according to many authors [2,3,7]. In this phase, as in the "Co(Ni)-Mo-S" phase, Ni atoms are adsorbed on the edges of WS<sub>2</sub> slabs, dispersed on the alumina support. However, there are other differences between Mo- and W-based catalysts i.e. the dif-

ferences in sulfidation behavior, inducing incomplete sulfidation for W and the influence of Co or Ni promoters, as reviewed by Hensen et al. [3]. Therefore, a different approach is needed in the synthesis of promoted tungsten sulfide catalysts, capable of taking full advantage of the promoter.

Regarding the synthesis of promoted sulfides, if conventional preparation methods are employed to synthesize promoted Co(Ni) Mo sulfides, i.e. incipient wetness impregnation of inorganic salts followed by sulfidation, the proximity of the involved metals cannot be generally controlled. This leads to the formation of segregated Ni<sub>x</sub>W<sub>y</sub> structures and to the loss of nickel atoms which migrate within the alumina matrix. However, due to the oxidative nature of the nitrate ion, an organic approach is preferred [8–10].

In an early work, the incorporation of the promoter was carried out by using a vapor deposition technique over sulfided MoS<sub>2</sub> as published by Angulo et al. [11]. In this work nickel carbonyl was successfully deposited on the MoS<sub>2</sub> slabs, as indicated by CO adsorption spectra. Moreover, in another study from Maugé et al. [12] a correlation between the characteristic band of adsorbed CO over promoted CoMoS site and the thiophene HDS rate constant, showed that the higher activity of the catalysts prepared with cobalt carbonyl nitrosyl was due to a greater ability of such complex to form promoted sites, as compared with a conventional catalyst. Similar studies afterwards [13–15], in which the precursor is a volatile carbonyl, have confirmed that the addition of cobalt or

\* Corresponding author.

E-mail address: [jarh@xanum.uam.mx](mailto:jarh@xanum.uam.mx) (J.A. De los Reyes).

nickel goes directly over the sulfided slabs of tungsten or molybdenum and a selective decoration of the slabs can be achieved. Because of the unstable precursors, an alternative technique was necessary.

A decade ago, a new procedure was developed by Bezverkhy et al. [9], which consists of a reflux of a  $\text{MoS}_2/\text{Al}_2\text{O}_3$  sample in a methanol solution of  $\text{Co}(\text{acac})_2 \cdot 2\text{H}_2\text{O}$ . Characterization by EXAFS showed that after such a treatment the Co atoms appeared in a sulfide environment. Thus, the catalytically active  $\text{CoMoS}$  phase was rapidly formed as the sample was heated to the reaction temperature. The “acac method”, that is, the use of the acetylacetone complexes over a sulfided phase in the preparation for  $\text{CoMoS}$  and  $\text{NiMoS}$  catalysts has also been studied by other authors. Roukoss et al. [8] evaluated the effect of using an organic precursor ( $\text{Co}(\text{acac})_2$ ) for the promoter in these catalysts on several supports. The catalyst supported on alumina prepared from cobalt acetylacetone doubled the activity in the HDS of thiophene when compared with the same catalyst prepared from an inorganic precursor ( $\text{Co}(\text{NiO}_3)_2$ ). Nihn et al. [16,17] obtained a similar result in the same reaction when they compared  $\text{NiMoS}$  catalysts supported on alumina, zirconia, titania and silica. These authors reported that alumina supported catalyst prepared from  $\text{Ni}(\text{acac})_2$  presented a 40% increment in the synergistic factor (defined as the ratio between the reaction rate of the catalyst with and without promoter) when compared with the same catalyst prepared from  $\text{Ni}(\text{NO}_3)_2$ .

Regarding other catalytic material, acetylacetones are widely used in nanoparticle tailoring and catalyst preparation due to their ability to modulate the reduction temperature of the complexed metal and because they can prevent the metal particles from forming large aggregates, thus allowing the metal to be better dispersed on a surface [18]. Furthermore, metal acetylacetones are often chosen in the synthesis of bimetallic catalysts, especially in the formation of alloys where the involved metals are different in nature [19,20]. Nevertheless, to our knowledge, we could not find any other reports on  $\text{NiW}$  sulfide catalysts by using acac compounds.

Taking into account the results for  $\text{NiMo}$  and  $\text{CoMo}$  catalysts, the impregnation of Ni over sulfided tungsten could allow both metals to be in close contact and thus, this could allow the promoter to be exploited and to increase the amount of  $\text{NiWS}$  phase in the final catalyst. Moreover, the effect of the solvent nature over the formation of an active phase in a hydrotreating catalyst has not been yet studied. Therefore, in this study, we selected four of the most available solvents, each with different properties, viz., methanol (polar), isopropanol (polar with steric hindrance), acetone (aprotic) and toluene (non-polar). We investigated the interaction between the promoter precursor and the solvent used and the effects of this interaction on the HDS catalytic reaction.

## 2. Experimental

### 2.1. Catalysts preparation

A starting material, named  $\text{W}/\text{Al}_2\text{O}_3$ , was prepared using the incipient wetness method. For this, a commercial  $\gamma$ -alumina ( $205 \text{ m}^2/\text{g}$ ) was impregnated with a solution of ammonium metatungstate (Aldrich) and kept overnight. The material was then dried at  $120^\circ\text{C}$  under static air for 2 h. W loading in this sample was 3 atoms/ $\text{nm}^2$  ( $\sim 14 \text{ wt.}\%$ ).

For the reference catalyst (NiW-Ref),  $\text{W}/\text{Al}_2\text{O}_3$  was impregnated with a nickel nitrate solution in water and kept overnight. The amount was enough to fill the pore volume. The solid was then dried under static air at  $120^\circ\text{C}$  for 2 h and sulfided at  $400^\circ\text{C}$  for 4 h. The loaded nickel atomic ratio ( $\text{Ni}/(\text{Ni} + \text{W})$ ) was of 0.3. The W and Ni contents for the NiW Ref catalyst were determined with Inductively Coupled Plasma (ICP) Chemical Analysis and they showed a

**Table 1**

Catalysts nomenclature and W and Ni loadings as determined by ICP chemical analyses.

Catalyst	solvent	W (wt%)	Ni (wt%)
NiW-a	acetone	13.2	1.6
NiW-t	toluene	13.2	1.6
NiW-i	isopropanol	14	1
NiW-m	methanol	14	0.9
NiW-Ref	–	14	1.6

fair agreement with the nominal loadings (14 wt.-% W and 1.6 wt.-% Ni).

For the acac method,  $\text{W}/\text{Al}_2\text{O}_3$  was sulfided for 4 h at  $400^\circ\text{C}$  under an  $\text{H}_2\text{S}/\text{H}_2$  mixture and then, the solid was kept under reflux of a solution of  $\text{Ni}(\text{acac})_2$  for 4 h at  $60^\circ\text{C}$ . The solvent in the reflux step was one of the following: acetone, toluene, 2-propanol (isopropanol) and methanol (Sigma-Aldrich; ACS Grade). The catalysts were named by using NiW followed by the initial of the solvent used in the promoter incorporation. The initial amount of Ni in all the reflux solutions per gram of catalyst was  $520 \mu\text{mol}$ . The amount of Ni deposited over the catalyst was determined from the decrease of the concentration in the solution, as determined by UV-vis spectroscopy using the band at 630 nm, which corresponds to the  ${}^3\text{A}_2 \rightarrow {}^3\text{T}_1({}^1\text{D})$  transition of nickel. The results were corroborated with Inductively Coupled Plasma (ICP) Chemical Analysis as shown on Table 1.

### 2.2. Hydrodesulfurization of 4,6-Dimethyldibenzothiophene

A batch reactor was used at  $320^\circ\text{C}$  and  $5.5 \text{ MPa}$  of  $\text{H}_2$  for 5 h for the hydrodesulfurization of 4,6 dimethyldibenzothiophene. Prior to the reaction experiments, the catalyst was again sulfided for 3 h at  $400^\circ\text{C}$ . Activity tests were performed as follows: About 120 mg of re-sulfided catalyst was immersed in a solution of 154 mg of 4,6-DMDBT (Sigma-Aldrich) in 100 ml of dodecane (Sigma-Aldrich). Precautions were taken so the catalyst had minimum contact with air and thus avoid re-oxidation of the active phase. Mass transfer limitations in the reactor were taken into account to determine appropriate kinetic regime conditions including particle size ( $\sim 150 \mu\text{m}$ ) and agitation speed (1000 rpm). Product analyses were performed using a Varian CP-3800 gas chromatograph equipped with a FID detector. A HP-5 column (5%-Phenyl-methylpolysiloxane) was used with helium as the carrier gas. High purity standards for all the compounds were used to identify the reaction products. The catalytic activity was expressed by the initial reaction rate (mol of 4,6 DMDBT transformed per second and per gram of catalyst). The specific reaction rate was defined in terms of the molecules converted per Ni atom per second:

$$r_s = \frac{rN}{n_{\text{Ni}}} \quad (1)$$

Where  $r$  is the overall initial reaction rate ( $\text{mol g}^{-1} \text{ s}^{-1}$ ),  $N$  is the Avogadro number and  $n_{\text{Ni}}$  is the amount of Ni (in atoms per gram of catalyst) determined from the change in concentration of the impregnation solution as explained in Section 2.1.

### 2.3. Characterization of materials

UV-vis analysis of the promoter incorporation and of saturated  $\text{Ni}(\text{acac})_2$  solutions were made with a Perkin Elmer Lambda 35 Spectrometer. For the liquid solutions, a 10 mm path cell was used and, for each sample, the solvent involved was used as reference. The solid  $\text{Ni}(\text{acac})_2$  was measured using diffuse reflectance spectroscopy with a Labsphere RSA-PE-20 accessory adapted to the previously described spectrometer. In order to obtain the position

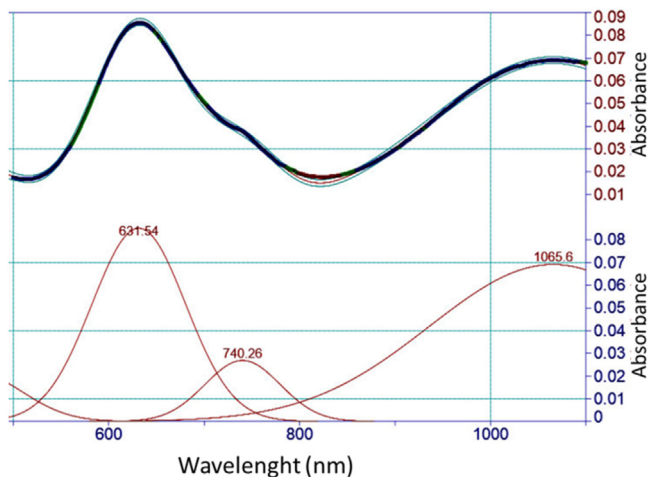


**Fig. 1.** Spectra for  $\text{Ni}(\text{acac})_2$  dissolved in methanol (top) and its decomposition assuming three visible transitions (bottom).

**Table 2**  
UV-vis Spectroscopy bands for saturated  $\text{Ni}(\text{acac})_2$  solutions in different solvents.

Transition	Wavelength (nm)	Methanol	Acetone	Isopropanol	Toluene	Solid $\text{Ni}(\text{acac})_2$ <sup>a</sup>
$^3\text{A}_2 \rightarrow$						
$^3\text{T}_1(^1\text{D})$	631.5	648.8	636.7	643.2	645.2	
$^1\text{E} (^1\text{D})$	740.2	769	756.5	743.6	761.8	
$^3\text{T}_2(^3\text{F})$	1065.6	>1100	1095.8	1048.6	1095.9	

<sup>a</sup> Diffuse reflectance.

of the maximum absorbance for each transition, the spectra were decomposed using PeakFit v4 software.

X-ray photoelectron spectroscopy analyses were performed on the samples prepared with toluene and with methanol before and after resultification in order to determine the influence of the solvent over the Ni and W species distribution. The technique was carried out under inert atmosphere using a KRATOS Analytical AXIS Ultra DLD spectrometer equipped with a Delay Line Detector. XPS measurements were taken with a monochromatized aluminum source (1486.6 eV). The C 1s binding energy was used for calibration (284.5 eV).

High resolution transmission electron microscopy (HRTEM) examinations were carried out with a JEOL 2010 (200 kV) instrument equipped with a Link ISIS microanalysis system. Its resolution was 0.195 nm. Previous to the HRTEM analysis, the samples were sulfided as described previously and kept under argon atmosphere to avoid air contact. Prior to analyses, the freshly sulfided samples were finely grounded, ultrasonically dispersed in ethanol and collected on a carbon-coated copper grid.

### 3. Results

#### 3.1. Nickel acetylacetonate solutions characterization

The spectroscopy characterization for 4 different solutions of nickel acetylacetonate was carried out in the visible spectral range (400–1100 nm) in order to determine the influence of the solvent on the Ni coordination. Fig. 1 gives an example of a typical spectrum for the Ni containing solutions and its Gaussian decomposition. A set of three bands was easily identified, corresponding to the expected transitions for a  $\text{Ni}^{2+}$  compound [21,22]. The transitions are represented according to the Mulliken symbols for molecular terms. The basal state for  $\text{Ni}^{2+}$  in  $\text{O}_h$  symmetry is  $^3\text{A}_{2g}(^3\text{F})$ . Table 2 summarizes the wavelength of the visible  $\text{Ni}(\text{acac})_2$  transitions when dissolved in methanol, isopropanol, toluene and acetone and the diffuse reflectance spectrum for the  $\text{Ni}(\text{acac})_2$ . For the solvents, only ace-

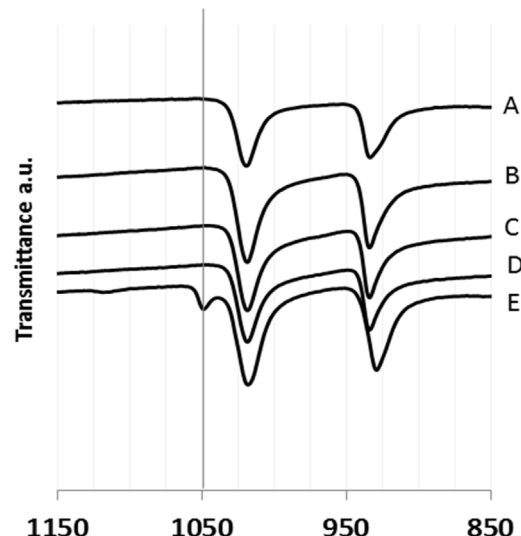


**Fig. 2.** ATR-FTIR spectra detail for  $\text{Ni}(\text{acac})_2$  as purchased (A) compared to the solid recovered after crystallization from the saturated solution in toluene (B), acetone (C), isopropanol (D) and methanol (E).

tone presented a shift towards a higher wavelength (bathochromic shift) when compared to the solid before dissolved, while a hypsochromic shift is noticeable for  $\text{Ni}(\text{acac})_2$  dissolved in toluene, methanol and isopropanol. According to Manch et al. [21], a shift towards the blue is expected when a ligand with a larger electrostatic field replaces the weak-field ligand. It is worth to notice that the shift of one band among two solvents is not equal to the shift of another band for the same solvents. According to this, the interaction between the metal and the ligand is different depending on its environment and thus, the general properties of the molecule are affected.

The saturated solutions were then evaporated at room temperature in order to obtain the nickel acetylacetonate in a solid state again. Depending on the solvent used, the size, color intensity and shape of the crystals were different. In order to understand the differences among the crystallized  $\text{Ni}(\text{acac})_2$ , we performed an FTIR scan of each solid and compared it with the commercial one. Based on the available literature [23–25] the identification of the peaks was possible. A complete tabulation of all absorption bands from  $550\text{ cm}^{-1}$  to  $1800\text{ cm}^{-1}$  is presented in Table 3. In all solids the bands were present at same proportions so decomposition of the complex was not favored in any solvent. The bands below  $700\text{ cm}^{-1}$  which correspond to the ring deformation and the metal oxygen interaction are only shifted towards lower frequencies in the case of the solid obtained from methanol. This is a good indicator that the intramolecular interactions are affected by this solvent. Also, a band at  $1049\text{ cm}^{-1}$  was noticed for this solid (Fig. 2). This band is usually associated to the C–O bond present in primary alcohols and surface methoxy groups [26] and is consistent with reported results where bis(acetylacetonato)dimethanolnickel(II)  $[\text{Ni}(\text{acac})_2(\text{MeOH})_2]$  was isolated and characterized [25].

#### 3.2. Reflux experiments for promoter incorporation

Fig. 3 depicts the evolution of the changes in Ni deposition on the solid for the various solutions. For each solvent, the Ni amount increases initially with reflux time and it reaches a stationary value above 100 min. However, even if the initial concentration of Ni was similar in all experiments, it can be seen in Fig. 3 that the amount of deposited Ni depends on the nature of the solvent. This amount of nickel deposited on the catalyst per gram of solid ( $q$ ) was estimated from the final Ni concentration in the solution. Reducing by a factor

**Table 3**

ATR-FTIR absorption bands in  $\text{cm}^{-1}$  for the solids obtained from saturated solutions of  $\text{Ni}(\text{acac})_2$  compared with the solid as purchased.

$\text{Ni}(\text{acac})_2$		Recrystallized from:			Assignment <sup>a</sup>
	Toluene	Acetone	Isopropanol	Methanol	
1653	1653	1653	1653	1654	$\nu(\text{C}=\text{C}-\text{O})$
1598	1597	1598	1598	1591	$\nu(\text{C}=\text{O})$ ; $\nu(\text{C}=\text{C})$
1517	1512	1512	1512	1513	$\nu(\text{C}=\text{O})$ ; $\gamma(\text{CH})$
1460	1462	1462	1460	1458	$\nu(\text{C}=\text{O})$ ; $\gamma(\text{CH})$
1396	1396	1396	1396	1400	$\delta(\text{CH}_3)$
1361				1364	$\delta(\text{CH}_3)$
1258	1262	1262	1262	1260	$\nu(\text{C}-\text{C}=\text{C})$ ; $\nu(\text{C}-\text{CH}_3)$
1202	1202	1201	1201	1197	$\delta(\text{CH})$
				1049	$\nu(\text{C}-\text{O})$
1019	1019	1018	1019	1018	$\rho(\text{CH}_3)$
934	934	934	934	929	$\nu(\text{C}-\text{CH}_3)$ ; $\nu(\text{C}-\text{O})$
766	766	765.5	765	766	$\gamma(\text{CH})$
674	674	674	674	673	$\Delta$ ; $\nu(\text{M}-\text{O})$
661	661	661	661	658	$\Delta$ ; $\nu(\text{M}-\text{O})$
590	589	588	589	587	$\Gamma$

<sup>a</sup>  $\nu$ , stretching;  $\delta$ , in plane bending;  $\gamma$ , out of plane bending;  $\rho$ , out of plane rocking;  $\Delta$ , in plane ring deformation;  $\Gamma$ , out of plane ring deformation.

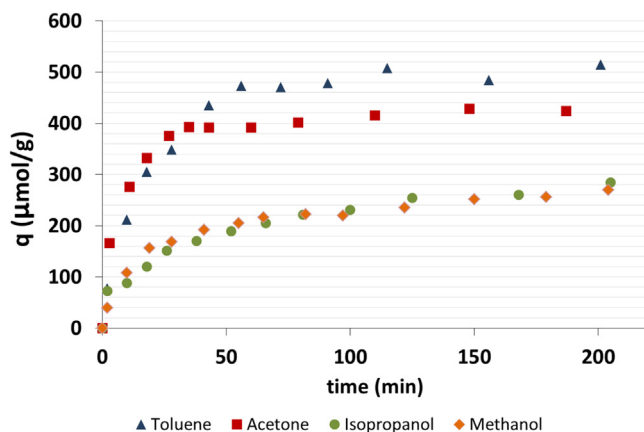


**Fig. 3.** Evolution of the amount of nickel deposited over the  $\text{WS}_2/\text{AlO}_3$  as calculated from reflux solutions versus time during the reflux for each solvent.

of two the initial concentration for a NiW-t sample leads to the same conclusion with a complete reaction of the Ni, therefore, toluene leads to a non-selective adsorption of the Ni whereas methanol does.

From curves in Fig. 3, one can deduce that the deposition rate for the alcohols (methanol and isopropanol) was somewhat similar and the concentration in the solution at the end was 50% of the initial one. For the toluene and acetone, the amount of nickel impregnated was 100% of the nickel available in solution. The amount of Ni estimated by UV-vis spectroscopy was confirmed by chemical analyses (induced coupled plasma) for two of the samples (NiW-m and NiW-t).

### 3.3. Catalytic activity

Fig. 4 gives the catalytic activities per gram of catalyst in the HDS of 4,6 DMDBT for the series of NiW catalysts (left side Y-axis). The catalysts prepared from nickel acetylacetone were up to 2.5 times more active than the reference catalyst prepared with nickel nitrate. The reaction rate for the latter was  $7 \text{ mol/g}_{\text{cat}} \text{ s}$ , while the reaction rates for the catalysts prepared with  $\text{Ni}(\text{acac})_2$  ranged from  $11.5 \text{ mol/g}_{\text{cat}} \text{ s}$  to  $17.5 \text{ mol/g}_{\text{cat}} \text{ s}$ . Among the catalysts prepared from nickel acetylacetone solutions, methanol and isopropanol solvents led to the highest reaction rate as compared to acetone and toluene.

Fig. 4 (right side axis) gives also the HDS activity based on the amount of nickel atoms deposited on the catalyst. Rates followed

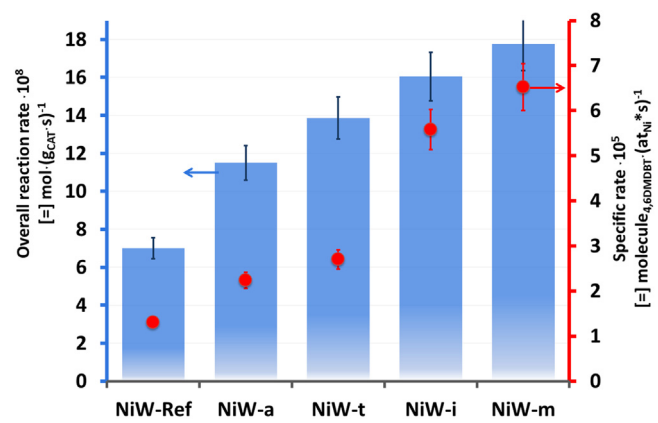


**Fig. 4.** Catalytic activity for supported  $\text{WS}_2$  catalysts using Nickel nitrate and  $\text{Ni}(\text{acac})_2$  dissolved in acetone, isopropanol, toluene and methanol, as promoter precursor.

the same increasing order, confirming the positive effect of this type of preparation. Nevertheless, the differences between the catalysts prepared from methanol and isopropanol were more significant when compared with the other three catalysts. Furthermore, the NiW-m catalyst exhibited a ca. 3-fold increase in the overall reaction rate as compared with the reference catalysts

The products of the reaction were consistent with the reaction scheme for the HDS of 4,6 DMDBT as reviewed previously [27] (and references therein), in which the removal of the heteroatom can take place either via two routes, namely: i) the direct removal of the sulfur atom (DDS) yielding 3,3'-dimethyl-biphenyl (DMBP) as product or ii) the hydrogenation (HYD) of the molecule previously to the C-S bond cleavage, yielding first the 4,6-dimethyl-1,2,3,4-tetrahydro-dibenzothiophene (4,6-DM-THDBT) and then 1-methyl-3-(3-methylcyclohexyl)benzene (also known as methylcyclohexyltoluene or MCHT) and 3,3'-dimethyl-1,1'-bi(cyclohexyl) (DMBCH). For all catalysts, the reaction proceeded mainly via the HYD route with MCHT as the main desulfurized product. The yield for the HYD path products was four times higher than the yield for DDS product.

### 3.4. Catalyst characterization

#### 3.4.1. X-Ray photoelectron spectroscopy (XPS)

The catalysts prepared from methanol and toluene solutions were analyzed using X-Ray photoelectron spectroscopy before (I)

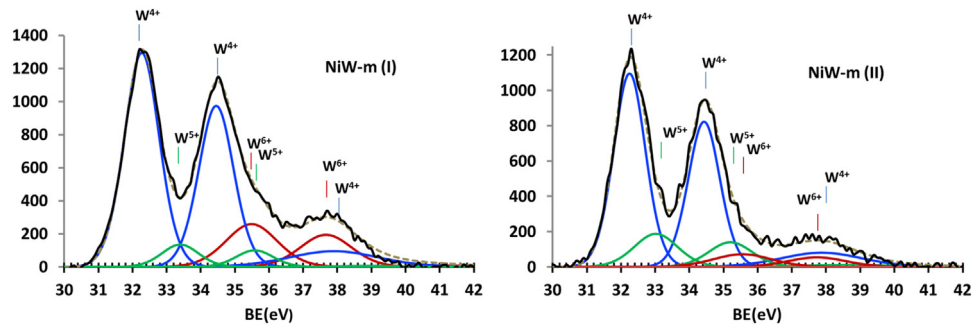


Fig. 5. XPS Spectra on the W4f region for the NiW-m catalyst after the reflux impregnation (I) and after resulfidation (II).

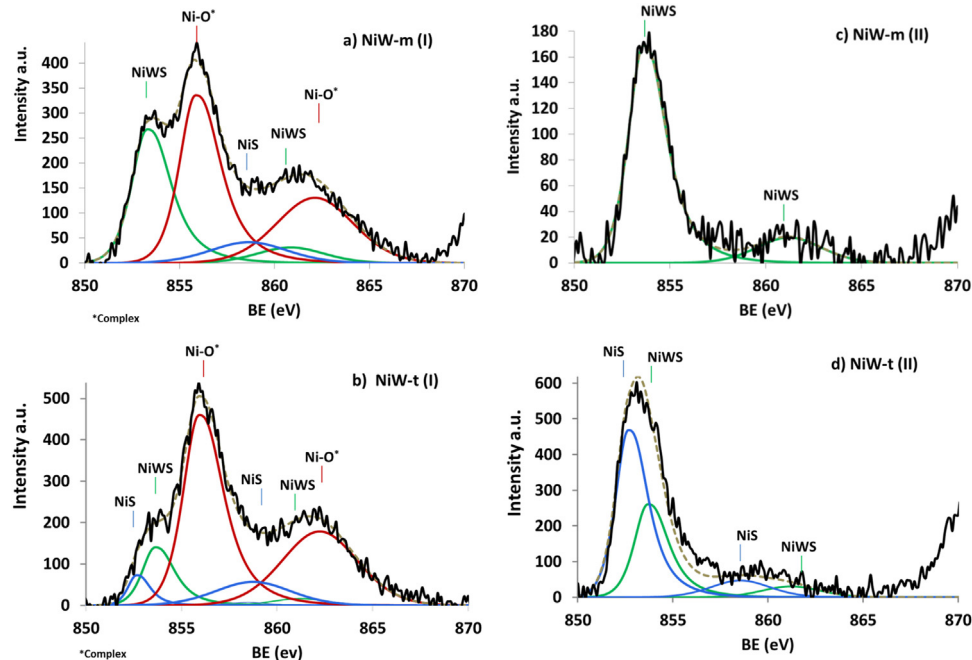


Fig. 6. XPS spectra on the Ni2p<sub>3/2</sub> region with deconvolution curves for NiW-m (a,c) and NiW-t (b,d) before (I) and after (II) resulfidation.

and after (II) resulfidation. A Gaussian decomposition was performed to the spectrum in order to identify the present phases of each element.

The W 4f region for the spectra between 32.3 eV and 37.7 eV exhibited the characteristic doublets for the 4f<sub>7/2</sub> and 4f<sub>5/2</sub> levels (Fig. 5). The obtained bands were decomposed in order to fit three species for each spectrum: a) at 32.3 eV for the W<sup>4+</sup> species, as in WS<sub>2</sub>; b) at 33.3 eV, associated with the intermediate oxysulfides W<sup>5+</sup> and c) at 35.5 eV, which correspond to W<sup>6+</sup> species, as reported for oxide species [28]. Since no significant changes were detected depending on the solvent, we provide one example for the W 4f region bands.

The sulfidation degree of tungsten, defined as the percentage of tungsten in the W<sup>4+</sup> oxidation state considering the total W species, can be calculated from the W 4f region of the spectra. For the catalyst impregnated with toluene, this parameter increased from 51.3% for sample NiW-t (I) to 81.6% for the sample NiW-t (II), whereas for the methanol impregnated sample, that parameter had no significant change after resulfidation (~73%).

The Ni 2p<sub>3/2</sub> region of the spectra is showed on Fig. 6. A characteristic feature of Ni among other transition metals is the tendency to present multiplet splitting associated to unpaired electron coupling and shake-up interactions [29]. The decomposition

and analysis of such interactions was beyond the reach of this work, thus, a single envelope was used to group them. As reference for the oxide contribution, bulk Ni(acac)<sub>2</sub> was analyzed and the resulting spectrum showed a main peak at 855.6 eV and a satellite envelope at 859.9 eV.

Fig. 6a) and b) gives XPS spectra in the Ni 2p<sub>3/2</sub> region for the catalysts after the impregnation with methanol and toluene and prior to sulfidation. The decomposition was made considering two potential Ni species: a) NiWS, square planar Ni interacting with the sulfidized phase of W (853.7 ± 0.5 eV) [30,31]; b) Ni(acac)<sub>2</sub> in interaction with the support (856 ± 0.5 eV) [16]. When using methanol as solvent, the Ni(acac)<sub>2</sub> band was at 855.8 eV and the NiWS band was at 853.5 eV. On the other hand, for the material prepared with toluene, the Ni(acac)<sub>2</sub> signal was at 856.0 eV and the one corresponding to the NiWS phase was at 853.9 eV. The energy shift of the precursor band is consistent with reported data [16]. These authors found similar values for catalysts with an interaction between acetylacetone with the support [16]. The relative quantities of the different Ni species which are present at the surface are given in Table 4. It can be observed that 32% of the impregnated nickel went directly to the edges of the WS<sub>2</sub> slabs in the reflux step when methanol was used as solvent; the remaining 68%

was still forming Ni–O bonds such as those present in the nickel acetylacetonate.

**Fig. 6c** and **d**) shows XPS spectra in the Ni 2p<sub>3/2</sub> region for the same catalysts as in **Fig. 6a**) and **b**) after sulfiding. It can be noticed that most of the nickel in the NiW-m sample was forming the NiWS phase (BE = 853.6 eV). For the catalyst prepared with toluene (NiW-t), Ni–S bonds, similar to those present in nickel sulfide (BE = 852.6 eV), were found constituting 62.5% of the Ni species; the balance was the NiWS phase.

#### 3.4.2. Transmission electron microscopy (TEM)

Representative micrographs for the a) NiW-t and b) NiW-m catalysts before resulfidation are presented in **Fig. 7**. For both materials, the typical WS<sub>2</sub> lamellar structures were observed. The observed spacing between the black lines (0.61 nm) matched with the interplanar spacing of the (002) basal plane in bulk WS<sub>2</sub> [32]. The length L and stacking number N of the slabs were measured for over 300 crystallites. In **Fig. 8**, the statistical distribution of the slabs is presented as well as the number of layers. It has to be noted that no difference was observed between the materials regarding these parameters. This result was expected due to the fact that the incorporation of the promoter was made over the tungsten sulfide phase, so the statistical analysis was performed using indistinctly both NiW-m and NiW-t. For the NiW-t catalyst, several regions of the material presented round particles with a size of 1.5–3 nm in diameter (**Fig. 8b**). The average stacking number and slab length were N = 1.82 and L = 5.02 nm respectively.

**Table 4**

Quantitative XPS analyses for NiWcatalysts on the Ni2p emission region. (I) before resulfidation (II) after resulfidation.

	NiS		NiWS		Ni–O (complex)	
	BE (eV)	%at.	BE (eV)	%at.	BE (eV)	%at.
NiW-t (I)	852.6	4.5	853.6	12.7	855.9	82.8
NiW-t (II)	852.7	62.4	853.9	37.5	–	–
NiW-m (I)	–	–	853.3	32.3	855.8	67.6
NiW-m (II)	–	–	853.6	100	–	–

## 4. Discussion

The aim of this work was to evaluate the effect of changing the solvent in the promotion of a supported WS<sub>2</sub> catalyst, using an organic Ni complex as a precursor. Our results confirmed that the HDS activity can be improved upon the election of the solvent. A series of catalyst was prepared using four common solvents with different polar properties via the “acac method”, namely: toluene, acetone, isopropanol and methanol. A solvatochromic effect was noted using spectroscopy analysis on saturated solutions of the organometallic compound, i. e. the response of the outer electrons of the Ni atom to an external excitation was different depending on the solvent used. Therefore, the bands were displaced.

The nephelauxetic parameter  $\beta$  and the orbital splitting parameter  $\Delta_0$  were obtained from the Tanabe Sugano diagram, according to the methodology described in [33]; to get a better understanding of the solvachromatic effect (see **Table 5**). It can be observed

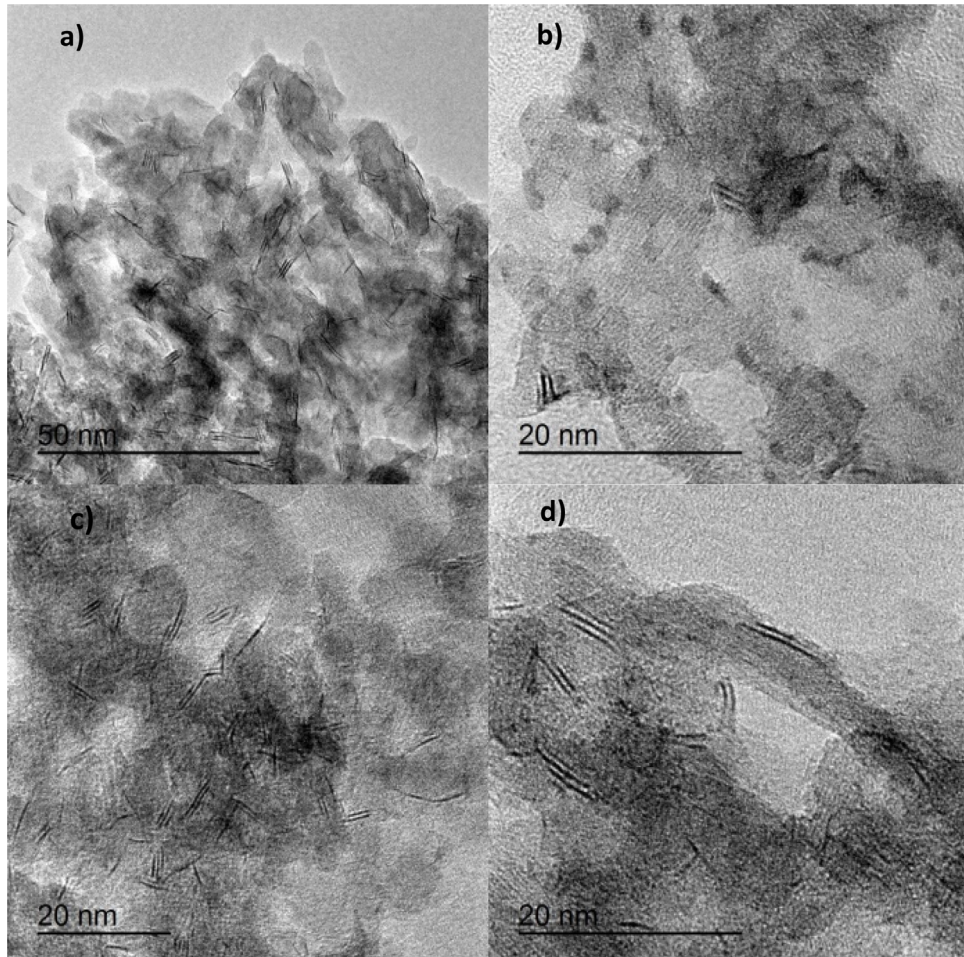


**Fig. 7.** Representative HRTEM images of (a,b) NiW-t (II) and (c,d) NiW-m (II).

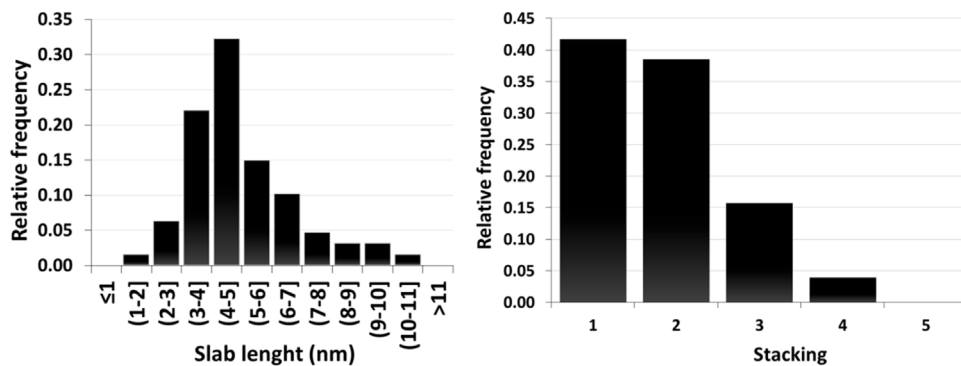


Fig. 8. Mean distribution of observed crystallite length and stacking number considering both NiW-t and NiW-m.

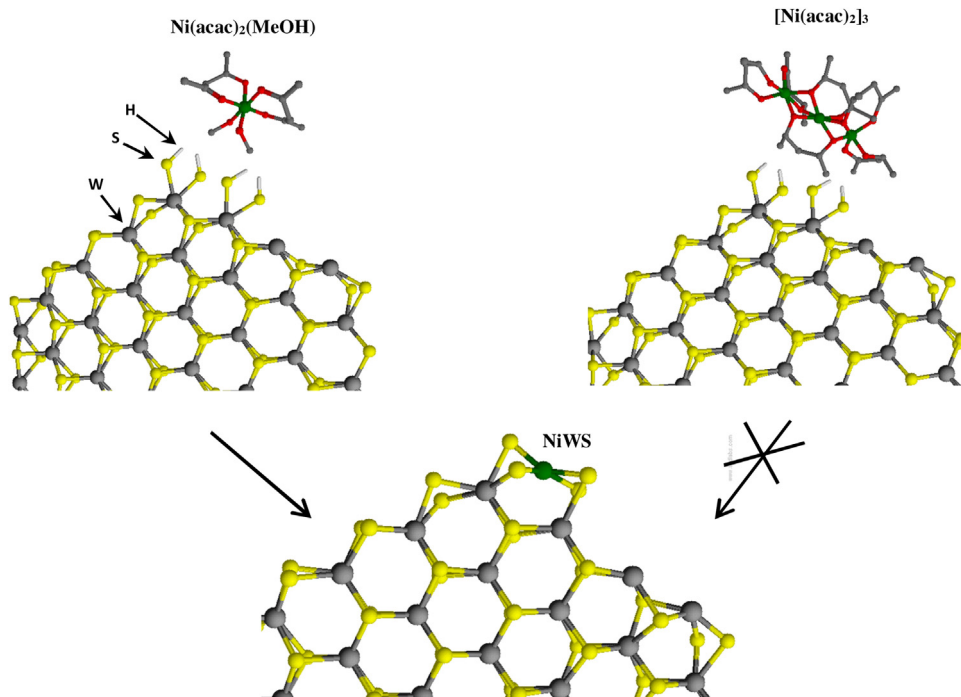


Fig. 9. Force Field representation of the mononuclear and the trinuclear forms of  $\text{Ni}(\text{acac})_2$  interacting with a  $\text{WS}_2$  slab edge.

from results in Table 5 that the acetylacetone complex had an effect over the outer electrons of the d-shell of Ni, given that the  $\beta$  parameter is inversely proportional to the size of the outer electron shell. This parameter has been associated with the metal polarizability and this property indicates the ability of the metal to react with soft bases [34,35]. However, these differences for the solvents were not significant to suggest a modification in the polarizability of the metal among the  $\text{Ni}(\text{acac})_2$  solutions.

Besides, the orbital splitting parameter, which represents the energy difference between the d orbitals facing the ligand and those which are geometrically farther and therefore, experience less repulsion, showed differences between the solvents of choice. The nickel ligands for the  $\text{Ni}(\text{acac})_2$  dissolved in methanol, had a more repulsive force over the d-shell electrons implying closeness to the metallic center. However, not only the outer electronic field of the metal was altered by changing the solvent but also the molecular structure of nickel acetylacetone can also be affected regarding the complex environment, as it has been mentioned before. The molecule forms a square planar and, thus, diamagnetic structure in vapor phase and when dissolved in high boiling point solvents above  $200^\circ\text{C}$  [23]. The trimeric form of the dehydrated solid  $[\text{Ni}(\text{acac})_2]_3$  was proposed by Bullen [36] in order to

Table 5  
Nephelauxetic parameter  $\beta$  and orbital splitting  $\Delta_o$  for the saturated solutions of  $\text{Ni}(\text{acac})_2$ .

	$\beta$	$\Delta_o$ ( $\text{cm}^{-1}$ )
Acetone	0.679	9680.1
Toluene	0.703	9703.0
Solid $\text{Ni}(\text{acac})_2$	0.686	9724.8
Isopropanol	0.690	9870.1
Methanol	0.706	9917.5

explain the paramagnetic nature of the metal. This structure was then confirmed years later [37]. In this trinuclear form, four oxygen atoms from the complex are forming a  $\mu_2$  bridging ligand between the metals, thus fulfilling the hexacoordinated nature of octahedral nickel. Dissolved in methanol, pyridine and ethanol, it forms a monomer with the octahedral coordination of Ni completed by two adducts of the alcohol [25,38,39]. At low concentrations of pyridine, a binuclear structure has been proposed to exist in equilibrium with the trinuclear form when dissolved in benzene [39]. Bipyridine, DMF and acetone have also been studied as solvents for nickel acetylacetone and a cis/trans isomerism has been found [40,41]. To date, it is unclear if there is a relationship between

these structures and the affinity of the organometallic for specific surface properties. Nevertheless, it is known that  $\text{Ni}(\text{acac})_2$  has a strong reactivity towards OH sites of the alumina surface [42,43]. In our case, sulfided materials have similar properties in which surface oxhydrol are replaced with sulphydrol groups. Moreover, it has been observed that relatively strong acid sites are located at the edge sites of the sulfided Mo/W slab for these catalysts. In that case, the affinity of the complex should be towards these sites, promoting the formation of a metal edge site, as proposed by Afanasiev [44]. Further work to get a deeper insight into these relationships is ongoing.

According to the XPS results, the amount of Ni forming the active NiWS phase after the reflux impregnation with methanol is 49% compared with the 35%, which is formed at the same conditions using toluene. This remarkable result is in good agreement with [9] where a reaction between nickel acetylacetone and the sulfided phase was predicted. After the sulfidation of the promoted catalysts (II), all of the Ni impregnated using methanol formed the NiWS phase while only 37.5% of the nickel impregnated with toluene formed the same phase; the balance was forming the inactive sulfide phase. If we take into account that the specific reaction rate reported in Fig. 6 for the NiW-t catalyst represents the 40% of the reaction rate of the NiW-m catalyst, we can assume that the difference in the activity for these materials is given only by the amount of Ni forming the NiWS phase. This result implies that the solvent used in the preparation of the catalyst does have an important influence in the path followed by the promoting metal at the time of its incorporation; the mononuclear form, as in methanol, readily reacts with the edge sulphydrol sites of the tungsten sulfide slab forming the NiWS phase, while the trinuclear species, as in toluene, present a hindrance of unknown nature (most likely steric), and thus, Ni forms the isolated NiS phase. It is well known from DFT calculations, that the promoter is tetracoordinated when it forms the NiWS phase [45], so in order to the acetylacetone to react with the edge sites, there must be four available sulphydrol groups for each Ni atom. Fig. 9 is a representation made with a force field software (ChemSketch;ACD/Labs) in order to illustrate such line of thought.

## 5. Conclusions

The  $\text{Ni}(\text{acac})_2$  based catalysts showed up to a 3-fold increase in the HDS of 4,6 DMDBT reaction rate when compared with the reference catalyst. Among the used solvents in the impregnation of the metal complex, methanol induced the highest specific activity, 130% higher than the catalyst prepared using toluene. According to the results presented in this study, the differences in activity shown by the catalysts synthesized from an organic precursor dissolved in different solvents may be related to the proneness of the nickel in the complex to form the NiWS active phase. The influence of the solvent over the Ni electronic environment and thus, over its affinity to different surface groups is an unexplored topic that seems to be essential in the synthesis of tailor-made catalysts in which the metals are fully exploited.

## Acknowledgment

Luis G. Woolfolk and José A. de los Reyes acknowledge CONACYT (México) for financial support though the scholarship No. 232097 and grant No. 237857.

## References

- [1] H. Topsøe, B.S. Clausen, F.E. Massoth, *Hydrotreating Catalysis*, Springer Berlin Heidelberg, Berlin Heidelberg, 1996.
- [2] Y. van der Meer, M.J. Vissenberg, V.H.J. de Beer, J.A.R. van Veen, A.M. van der Kraan, *Hyperfine Interact.* 139/140 (2002) 51–57.
- [3] E.J.M. Hensen, Y. van der Meer, J.A.R. van Veen, J.W. Niemantsverdriet, *Appl. Catal. A: Gen.* 322 (2007) 16–32.
- [4] D. Zuo, M. Vrinat, H. Nie, F. Maugé, Y. Shi, M. Lacroix, D. Li, *Catal. Today* 93–95 (2004) 751–760.
- [5] H. Li, M. Li, Y. Chu, F. Liu, H. Nie, *Appl. Catal. A: Gen.* 403 (2011) 75–82.
- [6] V.A. Suárez-Toriello, C.E. Santolalla-Vargas, J.A. de los Reyes, A. Vázquez-Zavala, M. Vrinat, C. Geantet, *J. Mol. Catal. A: Chem.* 404–405 (2015) 36–46.
- [7] S. Louwers, *J. Catal.* 139 (1993) 525–539.
- [8] C. Roukoss, D. Laurenti, E. Devers, K. Marchand, L. Massin, M. Vrinat, *Comptes Rendus Chim.* 12 (2009) 683–691.
- [9] I. Bezverkhy, P. Afanasiev, M. Lacroix, *J. Catal.* 230 (2005) 133–139.
- [10] Y. Ji, P. Afanasiev, M. Vrinat, W. Li, C. Li, *Appl. Catal. A: Gen.* 257 (2004) 157–164.
- [11] M. Angulo, F. Maugé, J.C. Duchet, J.C. Lavalley, *Bull. Soc. Chim. Belg.* 96 (2010) 925–930.
- [12] F. Mauge, A. Vallet, J. Bachelier, J. Duchet, J. Lavalley, *J. Catal.* 162 (1996) 88–95.
- [13] Y. Okamoto, S. Ishihara, M. Kawano, M. Satoh, T. Kubota, *J. Catal.* 217 (2003) 12–22.
- [14] J.L. Jung, H. Kim, H.K. Jae, A. Jo, S.H. Moon, *Appl. Catal. B: Environ.* 61 (2005) 274–280.
- [15] Y. Okamoto, *Bull. Chem. Soc. Jpn.* 87 (2014) 20–58.
- [16] T.K.T. Ninh, L. Massin, D. Laurenti, M. Vrinat, *Appl. Catal. A: Gen.* 407 (2011) 29–39.
- [17] T.K.T. Ninh, D. Laurenti, E. Leclerc, M. Vrinat, *Appl. Catal. A: Gen.* 487 (2014) 210–218.
- [18] S.Y. Tsareva, X. Devaux, E. McRae, L. Aranda, B. Gregoire, C. Carteret, M. Dossot, E. Lamouroux, Y. Fort, B. Humbert, J.-Y. Mevellec, N.Y. Carbon, (2014) 753–765.
- [19] A. Renouprez, K. Lebas, G. Bergeret, *J. Mol. Catal. A: Chem.* 120 (1997) 217–225.
- [20] N.M. Bertero, A.F. Trasarti, B. Moraweck, A. Borgna, A.J. Marchi, *Appl. Catal. A: Gen.* 358 (2009) 32–41.
- [21] W. Manch, W.C. Fernelius, *J. Chem. Educ.* 38 (1961) 192.
- [22] M.G. Brik, N.M. Avram, C.N. Avram, *Phys. B: Condens. Matter* 371 (2006) 43–49.
- [23] J.P. Fackler, M.L. Mittleman, H. Weigold, G.M. Barrow, *J. Phys. Chem.* 72 (1968) 4631–4636.
- [24] H.F. Holtzclaw, J.P. Collman, *J. Am. Chem. Soc.* 79 (1957) 3318–3322.
- [25] Ö. Metin, LT. Yıldırım, S. Özkar, *Inorg. Chem. Commun.* 10 (2007) 1121–1123.
- [26] L.J. Burcham, G. Deo, G. Xingtao, I.E. Wachs, *Top. Catal.* 11/12 (2000) 85–100.
- [27] F. Bataille, J.-L. Lemberton, P. Michaud, G. Péro, M. Vrinat, M. Lemaire, E. Schulz, M. Breysse, S. Kasztelan, *J. Catal.* 191 (2000) 409–422.
- [28] H.R. Reinhoudt, A.D. van Langeveld, R. Mariscal, V.H.J. de Beer, J.A.R. van Veen, S.T. Sie, J.A. Mouljin, *Stud. Surf. Sci. Catal.* 106 (1997) 263–271.
- [29] T. Novakov, R. Prins, *Solid State Commun.* 9 (1971) 1975–1979.
- [30] J.N. Diaz de León, M. Picquart, L. Massin, M. Vrinat, J.A. De Los Reyes, *J. Mol. Catal. A: Chem.* 363–364 (2012) 311–321.
- [31] V. Venkatachalam, K. Ramalingam, R. Akilan, K. Sivakumar, K. Chinnakali, Hoong-Kun Fun, *Polyhedron* 15 (1996) 1289–1294.
- [32] E. Payen, R. Hubaut, S. Kasztelan, O. Poulet, J. Grimblot, *J. Catal.* 147 (1994) 123–132.
- [33] J.E. House, *Inorganic Chemistry*, 1st ed., Academic Press, 2008, 2016, pp. 645–667.
- [34] S. Ahrlund, J. Chatt, N.R. Davies, *Q. Rev. Chem. Soc.* 12 (1958) 265.
- [35] R.G. Pearson, *J. Am. Chem. Soc.* 85 (1963) 3533–3539.
- [36] G.J. Bullen, R. Mason, P. Pauling, *Nature* 189 (1961) 291–292.
- [37] G.J. Bullen, R. Mason, P. Pauling, *Inorg. Chem. 4* (1965) 456–462.
- [38] C.E. Pfluger, T.S. Burke, A.L. Bednowitz, *J. Cryst. Mol. Struct.* 3 (1973) 181–191.
- [39] J.P. Fackler, *J. Am. Chem. Soc.* 84 (1962) 24–28.
- [40] M. Kudrat-E-Zahan, Y. Nishida, H. Sakiyama, *Inorganica Chim. Acta* 363 (2010) 168–172.
- [41] M.B. Hursthouse, M. a. Laffey, P.T. Moore, D.B. New, P.R. Raithby, P. Thornton, *J. Chem. Soc. Dalton Trans.* (1982) 307.
- [42] I.A. Ledenev, R.V. Prikhod'ko, I.V. Stolyarova, E.J.M. Hensen, J.A.R. van Veen, M.V. Sychev, V.V. Goncharuk, *Kinet. Catal.* 47 (2006) 451–459.
- [43] J.A.R. Van Veen, M.P.C. De Jong-Versloot, G.M.M. Van Kessel, F.J. Fels, *Thermochim. Acta* 152 (1989) 359–370.
- [44] P. Afanasiev, *J. Catal.* 269 (2010) 269–280.
- [45] M. Sun, A.E. Nelson, J. Adjaye, *J. Catal.* 226 (2004) 41–53.